Soil moisture information can improve shallow landslide forecasting using the hydrometeorological threshold approach

Marino, Pasquale; Peres, David J.; Cancelliere, Antonino; Greco, Roberto; Bogaard, Thom A.

DOI
10.1007/s10346-020-01420-8

Publication date
2020

Document Version
Final published version

Published in
Landslides

Citation (APA)
Marino, P., Peres, D. J., Cancelliere, A., Greco, R., & Bogaard, T. A. (2020). Soil moisture information can improve shallow landslide forecasting using the hydrometeorological threshold approach. *Landslides*, *17*(9), 2041-2054. https://doi.org/10.1007/s10346-020-01420-8

Original Paper

Landslides
DOI 10.1007/s10346-020-01420-8
Received: 12 December 2019
Accepted: 21 April 2020

Pasquale Marino · David J. Peres · Antonino Cancelliere · Roberto Greco · Thom A. Bogaard

Soil moisture information can improve shallow landslide forecasting using the hydrometeorological threshold approach

Abstract Empirical thresholds indicating the meteorological conditions leading to shallow landslide triggering are one of the most important components of landslide early warning systems (LEWS). Thresholds have been determined for many parts of the globe and present significant margins of improvement, especially for the high number of false alarms they produce. The use of soil moisture information to define hydro-meteorological thresholds is a potential way of improvement. Such information is becoming increasingly available from remote sensing and sensor networks, but to date, there is a lack of studies that quantify the possible improvement of the performance of LEWS. In this study, we investigate this issue by modelling the response of slopes to precipitations, introducing also the possible influence of uncertainty in soil moisture provided by either field sensors or remote sensing, and investigating various soil depths at which the information may be available. Results show that soil moisture information introduced within hydro-meteorological thresholds can significantly reduce the false alarm ratio of LEWS, while keeping at least unvaried the number of missed alarms. The degree of improvement is particularly significant in the case of soils with small water storage capacity.

Keywords Shallow landslide · Rainfall-induced landslide · Early warning system · Hydrological cause · Triggering rainfall event · Hydro-meteorological thresholds · Landslide hazard and risk management

Introduction

Forecasting rainfall-induced landslides is often entrusted to the definition of empirical thresholds (usually expressed in terms of rainfall intensity and duration) that link the precipitation to the triggering of landslides (Guzzetti et al. 2008). However, rainfall intensity-duration thresholds do not exploit the knowledge of hydrological processes that occur in the slope, so they tend to generate significant rates of false and missed alarms, reducing the credibility of landslide early warning systems (LEWS). Rainfall-induced shallow landslides usually occur in the initially unsaturated soil cover following an increase of pore water pressure, due to the increase of soil moisture, caused by large and persistent rainfall. So, this opens the possibility to use soil moisture in landslide research. Recently, Bogaard and Greco 2018 proposed the cause-trigger conceptual framework to develop hydro-meteorological thresholds that combine the antecedent causal factors and the actual trigger connected with landslide initiation. In fact, in some regions where rainfall-induced shallow landslides are particularly dangerous and pose a serious risk to people and infrastructures, the antecedent saturation is the predisposing factor, while the actual landslide triggering is associated with the hydrological response to the recent and incoming precipitation (Bogaard and Greco 2016).

Several studies introduced, directly or with models, the effects of antecedent soil moisture content in the empirical thresholds for improving landslide forecasting (Crozier 1999; Godt et al. 2006; Ponziani et al. 2012; Ciabatta et al. 2016; Segoni et al. 2018; Lazzari et al. 2018; Zhuo et al. 2019).

Soil moisture can be measured locally, by a range of on-site measurement techniques (Schmugge et al. 1980; Walker et al. 2004; Ochsner et al. 2013), or remotely, by satellites or airborne systems. On-site measurements have proved promising in improving the performance of thresholds for landslide early warning (Mirus et al. 2018; Zhao et al. 2019). On-site data are accurate but sparse, so there is an increasing interest on the possible use of remotely sensed data. And, in fact, recent research has shown that they can provide useful information for landslide prediction at regional scale, despite their coarse resolution and inherent uncertainty (Stähli et al. 2015; Brocca et al. 2016; Segoni et al. 2018; Thomas et al. 2019). Even at local scale, initial soil moisture derived from satellite data proved to improve the prediction of the movements of a large landslide (Brocca et al. 2012).

Remote sensing is the practice of acquiring information about the earth's surface through the acquisition of satellite images (Shravan Kumar Yadav and Roy 2013). Remote sensing soil moisture data are trustable, as showed in several studies comparing satellite data with hydrological modelling and on-site observations (Wagner et al. 2013; Peng et al. 2015; Ray et al. 2017; Ford and Quiring 2019). Certainly, remote sensing soil moisture data have a lower accuracy than field measurements (Al-Yaari et al. 2014), especially in steep terrain (Thomas et al. 2019) and owing to the presence of vegetation. Many satellites, placed in orbit in the past decades, some with the specific purpose of measuring soil moisture (e.g. Soil Moisture and Ocean Salinity (SMOS) by the European Space Agency, and Soil Moisture Active and Passive (SMAP) by the National Aeronautics and Space Administration), others including on board sensors providing estimates of soil moisture, such as the Advanced Scatterometer (ASCAT) on satellites MetOp-A and MetOp-B (Wagner et al. 2013), and the Advanced Microwave Scanning Radiometers, on satellites Aqua and Global Change Observation Mission-Water1 (Kawanishi et al. 2003), have proven successful for estimating global mapping of near-surface (0–5 cm) soil moisture at a spatial and temporal resolution, respectively, of 10–50 km and of 2–3 days (Rao et al. 1988; Schmugge 1998; Entekhabi et al. 2010; Kerr et al. 2012; Enrekhabi et al. 2014; Das et al. 2016; Mohanty et al. 2017; Lv et al. 2018). Recently, surface soil moisture products with enhanced spatial and temporal resolution (De Jeu et al. 2014; Parinussa et al. 2015) have been used in various water resources management, agricultural and flood early warning practices (Massari et al. 2014; Wanders et al. 2014; Li et al. 2016) .

This leads to the obvious question from scholars whether remotely sensed soil moisture information can be used to improve landslide hazard assessment and ultimately landslide early

Published online: 13 May 2020

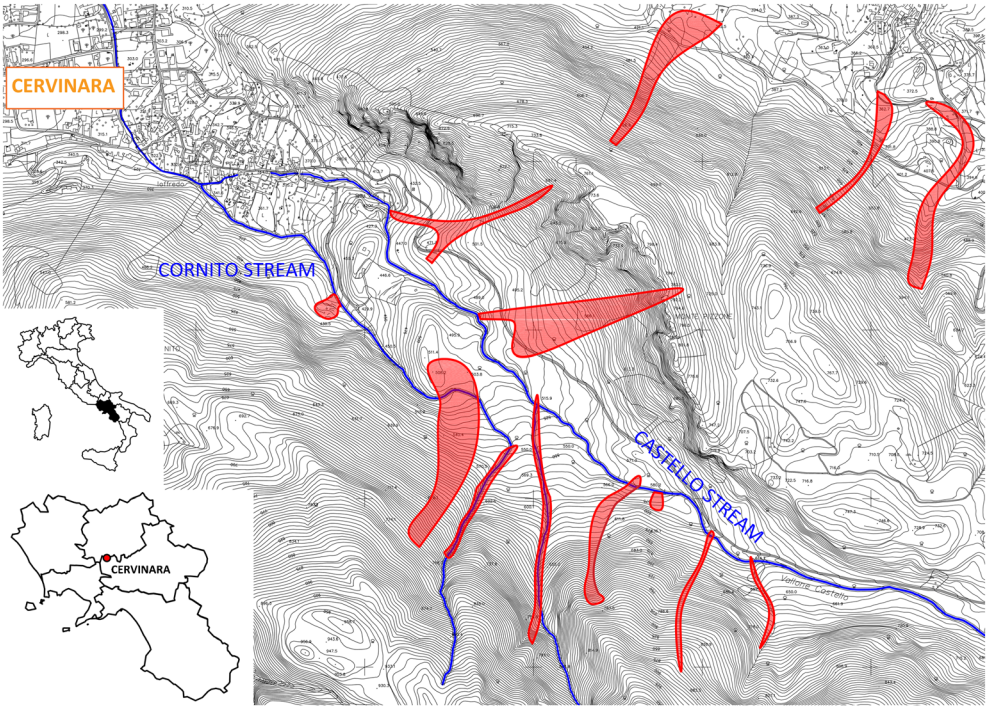

Fig. 1 Map of the test site of Cervinara (Campania, Southern Italy). The red zones represent the areas affected by debris flows triggered by a rainfall event of 325 mm in 48 h between 15 and 16 December 1999

warning systems (LEWS). Initiatives at global scale (Kirschbaum et al. 2009, 2012) down to regional and local scale (Brocca et al. 2016; Segoni et al. 2018) for using remotely sensed soil moisture for landslide hazard assessment are plentiful. Most of these applications use soil moisture products to obtain improved landslide susceptibility maps (Ray and Jacobs 2007; Ray et al. 2010). These maps can be used in conjunction with empirical landslide-triggering thresholds formulated in terms of rainfall intensity and duration (Kirschbaum et al. 2009, 2012).

However, the soil depth involved in a shallow landslide (the most prominent landslide type globally) is typically 1–2 m below the surface (Fiorillo et al. 2001; Greco et al. 2018), which is much thicker than the soil depth currently directly measured by remote sensing techniques, and in many cases overlaps with the root penetration depth. Such zone is influenced by antecedent precipitation, soil texture, vegetation, and therefore a clear relationship with near-surface soil moisture may be difficult to find. Many studies have attempted to derive root-zone soil moisture from near-surface moisture, through physically based approaches and data-driven methods (Kornelsen and Coulibaly 2014; Manfreda et al. 2014), data assimilation schemes (Walker et al. 2002; Sabater et al. 2007; Li et al. 2010; Dumedah et al. 2015; De Lannoy and Reichle 2016), and satellite information (Ragab 1995; Wagner et al. 1999; Miralles et al. 2011; Ford et al. 2014; Martens et al. 2017).

In our study, we address the question if soil moisture information, derived from current or future large scale monitoring products (e.g. either airborne and satellite remote sensing or diffuse sensor networks), can improve landslide hazard prediction, and to what extent. Hereto, we performed an explorative investigation based on real-world landslide and hydrological information from two areas in Southern Italy, both characterised by frequent shallow landslides, but with quite different geomorphologic features. To get data sets long enough to carry out statistical analyses, synthetic time series of rainfall and soil cover response have been generated for both sites, using a stochastic rainfall model and a physically based infiltration model.

Materials and methods

Synthetic data set generation

Aiming at comparing the landslide forecasting performances of empirical thresholds, based on rainfall information alone, with that of hydro-meteorological thresholds including also soil moisture information, a rich data set of rainfall, soil moisture, and landslides would be required. As the occurrence of landslides is usually not frequent enough to allow observing several landslide events within the duration of currently available rainfall records (i.e. some decades at maximum), in this study, a synthetic data set of the duration of 1000 years has been built with reference to two case studies, both characterised by the occurrence of rapid shallow landslides triggered by heavy rainfall.

This data set has been obtained by coupling a stochastic rainfall model with a physically based model of infiltration and drainage processes in the unsaturated slope cover (Peres and Cancelliere 2014, 2016, 2018). Specifically, a 1000 years hourly rainfall series has been generated with the Neyman-Scott Rectangular Pulse (NSRP) model (Neyman and Scott 1958), the parameters of which have been calibrated based on experimental data available at the investigated sites. The unsaturated flow modelling has been carried out using the vertical 1D Richards' equation, implemented in the HYDRUS-1D software (Šimůnek et al. 2008). In this case also, the

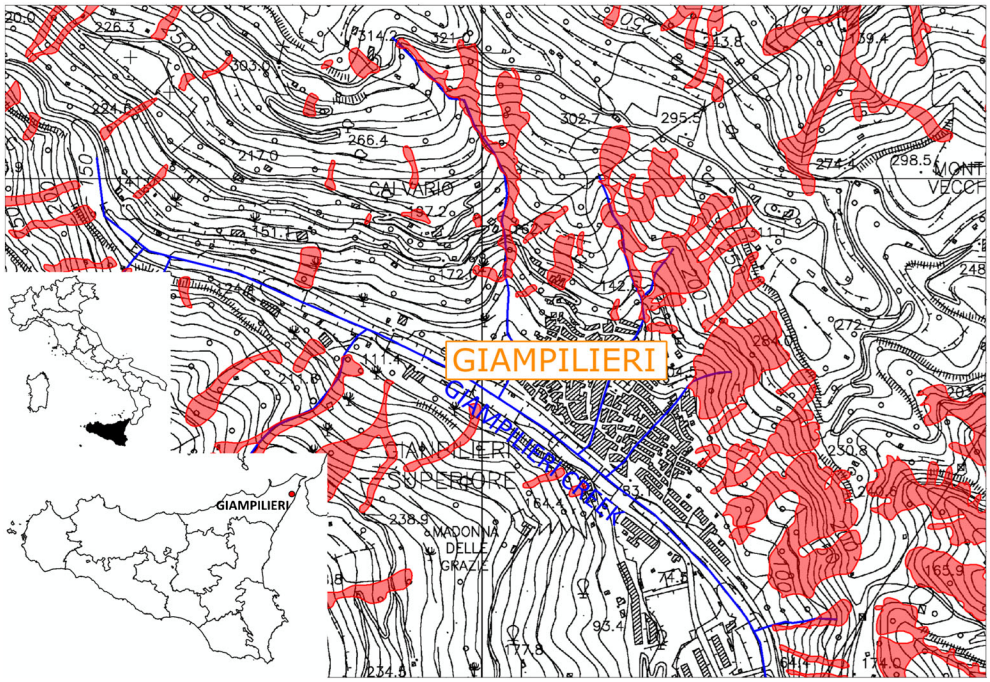

Fig. 2 Map of the test site of Giampilieri (Sicily, Southern Italy). The red zones represent the areas affected by debris flows triggered by a rainfall event of 220 mm in 7 h on 1 October 2009

parameters of the model have been assigned according to available laboratory and field observations at the investigated sites.

Case studies

The investigated areas, both located in southern Italy, are periodically affected by rainfall-triggered rapid shallow landslides. Specifically, the first case study refers to the slopes of the Partenio mountains, about 40 km north-east of Naples, Campania. The second case study is in Peloritani mountains, near Messina, Sicily. The two sites have been chosen for the investigation because of the different geomorphologic characteristics of the slopes, as well as for their climatic differences.

Campania

In Campania, many mountainous areas are covered with shallow volcanoclastic deposits, usually in unsaturated conditions, derived from the activities of two volcanoes (Somma-Vesuvius and Phlegrean Fields) during the last 40,000 years (Rolandi et al. 2003). Mesozoic-Cenozoic fractured limestones represent the basal rock, in which large karst aquifers are present, and the covers are mainly constituted by layers of coarse pumices, volcanic ashes, finer pumices mixed with ash, and altered ashes, the latter often observed near the soil-bedrock interface. The study area is along the slopes of Mount Cornito, near the town of Cervinara, at the base of the northern side of the Partenio mountains. The slope was involved in a series of landslides evolving in the form of fast flows, after a rainstorm of 325 mm in 48 h, in the night between 15 and 16 December 1999, causing the death of six people and heavy damages (Fiorillo et al. 2001). A map of the area, with indication of the occurred landslides, is given in Fig. 1.

The slope of Cervinara has an average inclination around 40° and is located at an elevation between 500 m and 800 m a.s.l. The thickness of the volcanoclastic soil cover is between 2 and 2.5 m, and it consists of an alternation of loose volcanic ashes (sand to loamy sand) and pumices (sandy gravel), lying upon a fractured limestone bedrock. The soils are characterised by high porosity (i.e. up to 0.75 for the ashes, around 0.5 for the pumices) and very high saturated hydraulic conductivity (i.e. in the order of 10^{-5}–10^{-4} m s^{-1} for the ashes, and even higher for the pumices). The soil-bedrock interface is pervious, and the leakage supplies both shallow and deep groundwater circulation (Allocca et al. 2014; Greco et al. 2018). Hence, the soil cover has high water retention capacity and allows for rapid infiltration and drainage processes. The climate is Mediterranean, with mean annual precipitation and potential evapotranspiration, respectively, of about 1600 mm and 750 mm, this latter estimated with the empirical formula of Thornthwaite (Shuttleworth 1993). The vegetation cover mainly consists of deciduous woods, mostly chestnuts, with a dense underbrush developing in spring and summer.

Sicily

Peloritani mountains in Sicily extend for about 65 km from Capo Peloro to Nebrodi, reaching the height of 1300 m. The mountains represent the inside chain of the Apennine–Maghrebian domain belonging geologically to the Calabrian-Peloritani Arc (Bonardi et al. 2002; Vignaroli et al. 2008). The geology of the area is characterised by a metamorphic bedrock (phyllites, schists, and paragneiss) with few and small outcrops of sedimentary deposits (marls, clays, and calcarenites). For our study, we consider the upper Ionian part of the Peloritani mountains, in the vicinity of the town of Giampilieri. On 1 October 2009, deadly landslides were triggered in this area, by a rainfall event of more than 220 mm in 7 h (Maugeri and Motta 2011; Ardizzone et al. 2012; Stancanelli

Table 1 Seasonally calibrated parameters of the NSRP model of rainfall for the two test sites

Rain gauge	Cervinara (Campania)						
Season	September	October	November	December–March	April	May–June	July–August
λ (h^{-1})	0.0150	0.00524	0.00257	0.0238	0.00809	0.00386	0.00900
ν	2.684	36.4	57.1	2.601	38.7	21.6	1.396
β (h^{-1})	0.265	0.156	0.0167	0.813	0.123	0.116	24.5
η (h^{-1})	1.411	57.3	1.430	0.280	15.5	8.59	1.231
ξ (h^b mm^{-b})	0.330	0.0471	0.450	0.967	0.186	0.158	0.268
Rain gauge	Fiumedinisi (Sicily)						
Season	September–October		November	December	January–March		April–August
λ (h^{-1})	0.0212		0.00149	0.00319	0.00230		-
ν	1.57		42.4	42.6	44.3		-
β (h^{-1})	2.12		0.00596	0.00988	0.0102		-
η (h^{-1})	0.840		0.941	0.677	0.721		-
ξ (h^b mm^{-b})	0.463		0.693	1.035	1.134		-

et al. 2017). Figure 2 below shows a map of the area, with the landslides occurred on that occasion.

The unstable slopes in the area are mostly in the range 35–45°, and the thickness of the heterogeneous, loose, and weathered layer covering the fractured metamorphic bedrock is 1.5–2.5 m. The soil has a high coarse fraction (gravel content more than 50%) and a scarce clay content; porosity is around 0.35–0.45, and saturated hydraulic conductivity in the order of 10^{-5} m s^{-1} (De Guidi and Scudero 2013; Peres and Cancelliere 2014; Schilirò et al. 2015). Climate in the Peloritani area is Mediterranean, with hot and dry summers, and precipitation, mainly convective, falls mostly in the period from October to January; mean annual precipitation and potential evapotranspiration (estimated by Thornthwaite formula) are, respectively, of about 1000 mm and 800 mm. A significant proportion of the soil is almost bare; otherwise, Mediterranean scrub is present, and only sparse areas are covered by trees (olive, oak, and beech).

Identification of parameters of the models

Rainfall generator

The NSRP stochastic model reproduces the point precipitation process as a series of rain clusters (i.e. rain storms), composed by a random number C of (possibly overlapping) rain cells, each schematised as a rectangular pulse with random duration and constant intensity, so that the total intensity is the sum of the intensities of contemporary active cells (Neyman and Scott 1958; Rodriguez-Iturbe et al. 1987; Cowpertwait et al. 1996). The arrival time of the clusters follows a Poisson distribution with parameter λ [T^{-1}]. Also, the number of cells within a cluster follows a Poisson distribution with mean ν [−]. The time of origin of each cell (elapsed from the beginning of the cluster) is exponentially distributed with parameter β [T^{-1}]. Rectangular cell duration and intensity have, respectively, exponential distribution, with parameter η [T^{-1}], and Weibull distribution, with cumulative probability function $F(x) = 1 - \exp(-\xi x^b)$, with the parameter b [−] set to 0.8 for Partenio mountains and to 0.6 for Peloritani mountains, and the parameter ξ [$T^b L^{-b}$] to be calibrated. In total, five parameters need to be identified, and model calibration was carried out with the method of moments, i.e. solving the system of equations with the expressions of the first five moments and minimizing a measure of the difference between theoretical and sample moments (Peres and Cancelliere 2014). The parameters of the NSRP model of rainfall were calibrated, for both the investigated sites, based on available rainfall records. Specifically, data from the rain gauge station of Cervinara, belonging to the Italian civil protection meteorological alert network, available from 1 January 2001 to 31 December 2017 with time resolution of 10 min, were used for the case study of Partenio mountains, Campania. For Peloritani mountains, Sicily, the available rainfall data set, with hourly resolution, belongs to the rain gauge station of Fiumedinisi and spans from 1 May 2002 to 31 December 2013. In Cervinara, the mean annual precipitation is 1600 mm, and, although autumn and spring are the rainiest seasons, it normally rains throughout the whole year (Comegna et al. 2016). In Giampilieri, instead, the mean annual precipitation is about 1000 mm, and the summers are usually almost dry, being intense or prolonged rainfall events between April and August extremely rare (Cama et al. 2015). To account for the seasonality, typical of Mediterranean climate, the experimental data sets were split in subsets corresponding to the periods of the year when precipitations showed homogeneous characteristics. The statistically homogeneous

Table 2 Parameters of the unsaturated flow model for the two test sites

Case study -	θ_s -	θ_r -	K_s m h^{-1}	d m	a m^{-1}	α °	m –	n –	A_{qh} m h^{-1}	B_{qh} m^{-1}	h_0 m
Cervinara	0.75	0.05	0.29	2.5	12	40	0.31	1.45	− 0.0107	− 6.0	0
Giampilieri	0.35	0.045	0.072	2.5	4	40	0.5	2	− 0.0145	− 2.085	2

periods were chosen by estimating the monthly values of the moments required for model calibration and then grouping the adjoining months which presented similar values of the moments. In such a way, five homogeneous periods were identified for Fiumedinisi and seven periods for Cervinara. Table 1 summarises the obtained parameters. It is worth to note that, for the rain gauge of Fiumedinisi, the period from April to August presented so few rainfall events that it could be considered dry for the purposes of this study, and thus the NSRP model was not calibrated and no synthetic rainfall data were generated for that part of the year.

The calibrated models were used to generate 1000 years long synthetic hourly rainfall series, the reliability of which was tested by calculating several statistics (e.g. annual rainfall, yearly number of storms, storm durations, and mean intensities) from randomly extracted subsets of the same duration of the experimental ones used for calibration (i.e. respectively, 17 years for Cervinara and 11 years for Fiumedinisi), and comparing their distributions with those of the experimental data.

Unsaturated flow model

As in the considered shallow unsaturated soil covers only occasionally subsurface downslope flow components occur (i.e. only whereas a nearly saturated condition is attained somewhere in the cover), the modelling of the flows, through the unsaturated soil cover of thickness d [L], was carried out using the 1D Richards' equation (Richards 1931). To such aim, the HYDRUS-1D software was used (Šimůnek et al. 2008). More specifically, the infiltration equation is as follows:

$$\frac{\partial \theta}{\partial t} = \frac{\partial}{\partial z}\left[K_s\left(\frac{\partial \psi}{\partial z} + \cos\alpha\right)\right] - S \tag{1}$$

where ψ is pore pressure head [L], θ is soil volumetric water content [$L^3\ L^{-3}$], z is the space coordinate orthogonal to slope surface [L], α [rad] is the angle of slope inclination respect to the horizontal, K_s is the unsaturated hydraulic conductivity function [$L\ T^{-1}$], and $S = \rho(\psi)S_p$ is the root water uptake [$L^3\ L^{-3}\ T^{-1}$], $\rho(\psi)$ being the dimensionless water stress response function of water potential ($0 \le \rho \le 1$), and S_p the potential water uptake rate [T^{-1}], depending on potential evapotranspiration and root distribution within the soil profile (Feddes et al. 1976). The soil water characteristic curves (SWCC) were expressed with the van Genuchten–Mualem model (van Genuchten 1980):

$$\theta(\psi) = \begin{cases} \theta_r + \dfrac{\theta_s - \theta_r}{\left[1 + |a\psi|^n\right]^m} & \psi < 0 \\ \theta_s & \psi \ge 0 \end{cases} \tag{2}$$

$$K(\psi) = K_s S_e^l\left[1 - \left(1 - S_e^{1-m}\right)^m\right]^2 \tag{3}$$

where θ_r is residual soil volumetric water content [$L^3\ L^{-3}$], θ_s is saturated soil volumetric water content [$L^3\ L^{-3}$], a, n, and $m = 1 - 1/n$ are the SWCC parameters, K_s [$L\ T^{-1}$] is the saturated hydraulic conductivity, and $S_e = (\theta - \theta_r)/(\theta_s - \theta_r)$ [−] is effective saturation. The leakage component at the soil-bedrock interface is approximated by the following equation:

$$q(h) = -A_{qh}\exp\left(B_{qh}|\psi - h_o|\right) \tag{4}$$

where A_{qh} and B_{qh} are empirical parameters, and h_o [L] is the position of the groundwater level with respect to the base of the soil cover.

For the case study of Cervinara, the parameters of SWCC have been assigned based on laboratory measurements (Greco et al. 2010; Damiano and Olivares 2010) and field monitoring data (Damiano et al. 2012; Greco et al. 2013; Comegna et al. 2016). The parameters of the leakage exponential relationship (4) have been adjusted in such a way to have water potential fluctuations, near the base of the cover, comparable with those observed in the field, where, at the depth of around − 1.80 m, the potential drops to − 10 m or less in summer, while it rises to more than − 1.0 m in winter (Damiano et al. 2012; Comegna et al. 2016). In the case of Giampilieri (Peloritani mountains), as no direct measurements of water retention nor hydraulic conductivity were available, the van Genuchten parameters were estimated from measured grain size distributions via the program ROSETTA, based on pedo-transfer functions (Schaap et al. 2001; Peres 2013). Regarding the parameters A_{qh} and B_{qh} of the bottom leakage function (4), they were adjusted within the range of values consistent with the actual hydraulic behaviour of the fractured bedrock, so to reproduce as closely as possible the four dates of past observed slope failures. In Table 2 below, the parameters adopted for the two case studies are reported.

Empirical landslide thresholds

Two different types of empirical thresholds have been defined to assess the potential improvement that the inclusion of moisture content information, prior the rain event, may determine in the capability of predicting landslide initiation. Specifically, the precipitation intensity-duration threshold is compared with two hydro-meteorological thresholds. The meteorological variable is in both cases the event precipitation depth, while the hydrological variable is either the near-surface soil moisture θ_{NS} (i.e. the average water content of the upper 5 cm of soil, provided by currently available remote sensing techniques), or the root zone soil moisture θ_{RZ} (here conventionally assumed as the average water content of the upper 100 cm of soil, which to date can be achieved by field sensors). To define these thresholds, a rainfall event is considered triggering when at least one landslide occurs during its course or after its end, but before the beginning of the following rainfall event. The information about prior soil moisture refers to a time interval before the beginning of the rainfall event, which depends on the hypothesised frequency of acquisition of soil moisture measurements.

Definition of rainfall events

The identification of possible cause-effect relationships, linking rainfall and soil moisture to landslides, requires the definition of rainfall events within the 1000 years long generated rainfall series. To this aim, a minimum inter-event time interval of 24 h has been introduced, characterised by a rainfall depth smaller than 2.0 mm (i.e. rainfall smaller than the mean daily potential evapotranspiration) (Peres et al. 2018). Hence, the obtained rainfall events were periods with at least 2.0-mm rainfall depth, preceded and followed by at least 24 h with less than 2.0-mm rainfall. Table 3 summarises some major statistical characteristics of the obtained series of rainfall events.

Rainfall events in Giampilieri are less frequent and longer than in Cervinara. The variability of both duration and intensity is smaller in Cervinara than in Giampilieri, where the maximum values of mean event rainfall intensity are attained.

Definition of landslide triggering condition

Landslide triggering conditions are defined as a limit value of pore water pressure, chosen according to the geotechnical characteristics of the soil constituting the cover. In both the test sites, the potential failure surface has been assumed at the depth of 2.0 m below the ground surface, and the critical water pressure height, ψ_c, corresponding to landslide triggering, has been defined so to have $F_s \sim 1$ with a uniformly wet soil profile.

The considered 1-D geometry of the soil cover allows the assumption of the infinite slope hypothesis for the evaluation of the factor of safety:

$$F_s = \frac{\tau_{lim}}{\tau'} = \frac{c' + \gamma d_f \cos^2\alpha \tan\phi' - \chi(\psi)\gamma_w \psi \tan\phi'}{\gamma d_f \sin\alpha \cos\alpha} \quad (5)$$

In Eq. 5, α [−] is the slope inclination angle, d_f [L] is the vertical depth, below the ground surface, at which the factor of safety is evaluated, γ [$M\,L^{-2}\,T^{-2}$] is soil unit weight, γ_w [$M\,L^{-2}\,T^{-2}$] is water unit weight, ϕ' [−] and c' [$M\,L^{-1}\,T^{-2}$] are, respectively, effective friction angle and cohesion of the soil, and χ [−] is Bishop's coefficient for the calculation of the effects of pore water pressure on soil shear strength (Bishop 1959). At saturation, it is $\chi = 1$, while in unsaturated conditions, the simplified assumption $\chi = S_e$ (Lu et al. 2010) has been made, as it seems acceptable for granular soils (Greco and Gargano 2015). Table 4 gives the geotechnical properties of the soils at the two test sites (Damiano and Olivares 2010; Peres and Cancelliere 2014), the major geometrical characteristics of the two slopes and the corresponding critical pore water pressure height.

The results of the unsaturated flow model ("Unsaturated flow model" section) show that the critical pressure height was overcome 231 times in 1000 years in Giampilieri (Sicily), which is consistent with the return period of landslides in Peloritani mountains along slopes inclined at 40°, i.e. about 5 years, estimated by (Peres and Cancelliere 2016). In Cervinara (Campania), instead, 42 landslide triggering events occurred along the 1000 years long simulation, corresponding to a return period of about 25 years, which appears consistent with the historical occurrence of landslides in other similar contexts of Campania (Bisson et al. 2007; Papa et al. 2011).

Table 3 Major characteristics of the rainfall events belonging to the 1000 years long synthetic rainfall series in the two test sites

Test sites	No. of events	Duration (h)					Intensity (mm h^{-1})			
		Min	Max	Mean	St. dev.	Median	Min	Max	Mean	St. dev.	Median
Cervinara	53061	1	570	19.3	24.7	12	0.09	91.8	2.67	3.75	1.63
Giampilieri	24492	1	685	32.9	45.6	17	0.09	179.4	4.49	8.33	1.29

Table 4 Major geotechnical and geometrical characteristics, and critical pore water pressure height, corresponding to landslide triggering, at the two test slopes

Test sites	Soil dry unit weight, γ_{dry} (N m^{-3})	Soil effective cohesion, c (kPa)	Soil effective friction angle, φ′ (°)	Failure surface depth, d_f (m)	Slope inclination angle, α (°)	Critical pressure height, ψ_c (m)
Cervinara	6500	0	38	2.0	40	−0.16
Giampilieri	15600	5.7	37	2.0	40	0.51

Definition of empirical thresholds for landslide initiation

Rainfall events are represented in the plane (D, I) for the identification of intensity-duration (meteorological) threshold, and in the planes (θ_{NS}, H) and (θ_{RZ}, H) to define hydro-meteorological thresholds. The thresholds are power-law equations (i.e. $Y = A\ X^B$) separating rainfall events with landslides from those without, and the parameters A and B are identified by maximizing the true skill statistics T [−] (Peirce 1884), a measure of the performance of the threshold which considers both missed alarms and false alarms:

$$T = 1 - \frac{M}{P} - \frac{F}{N} \quad (6)$$

In Eq. (6), M represents the number of missed alarms (i.e. events not exceeding the thresholds, but associated with the occurrence of a landslide), P the total number of occurred landslides, F the number of false alarms (i.e. events exceeding the threshold, but without the occurrence of any landslide), N the total number of rainfall events which are not followed by any landslide. $T = 1$ indicates a threshold which makes no error, $T = 0$ a random prediction, and $T = -1$ a threshold that yields systematically inverted predictions. Considering also the false alarms in the definition of the threshold avoids producing the well-known cry-wolf effect (Breznitz 1984), caused by a system launching too many alarms not followed by any landslide. It is worth to note that, when dealing with phenomena so rare as rainfall-induced landslides along a slope, it is always $N \gg P$; thus, the value of T is more sensitive to missed alarms than to false alarms.

Results and discussion

Meteorological threshold

In Fig. 3, the scatterplots of the triggering (red points) and non-triggering (blue points) rainfall events of Cervinara and Giampilieri are shown in the log-log plane of rainfall duration and intensity. In both the graphs, a power-law threshold curve has been drawn, defined by maximization of T (Eq. (6)).

For Cervinara (Fig. 3a, Table 5), the obtained threshold ($I = 175.56\ D^{-1,\ 08}$) performs excellently, as denoted by the value of $T = 0.934$. Interestingly, the long triggering events (with $D > 100$ h) are arranged in a less inclined way than the linear threshold line, which implies that more rainfall is required to trigger landslides. This is consistent with the fact that rainfall average intensity tends to decrease with longer durations and therefore the drainage of the infiltrating water plays a more significant role. The meteorological I-D landslide threshold correctly identifies nearly all the landslides, occurring about once every 25 years, but it yields nearly one false alarm per year. Although the missed alarms are very few (5% of the total number of predicted landslides, 2 of 42), the question arises whether people would still trust the warning messages launched by a LEWS based on the threshold, which issues so many alarms not followed by a landslide.

For Giampilieri (Fig. 3b), the optimal I-D threshold is $I = 73.3\ D^{-1,\ 0}$ but it suffers both false and missed alarms (Table 5). The threshold correctly predicts more than 85% of the landslides, but also in this case, people would experience around 15 false alarms on every single true alarm. Considering that missed alarms would also be, on average, once every 30 years, also for Giampilieri,

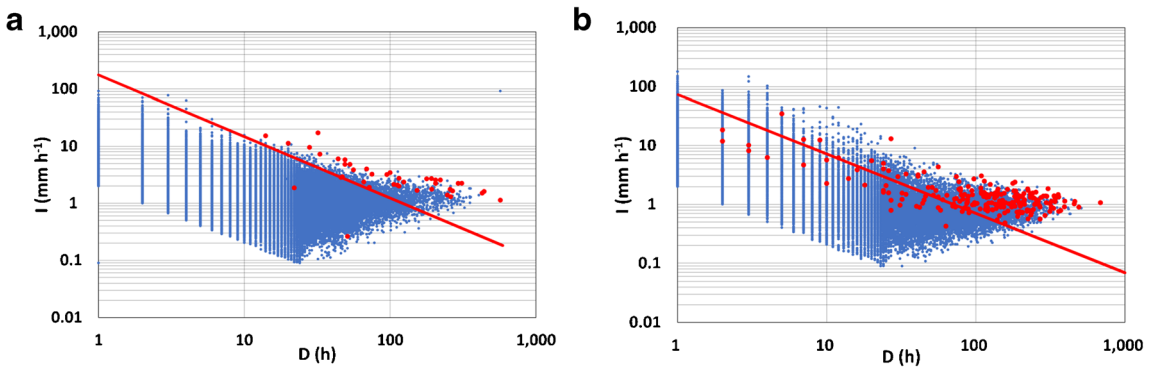

Fig. 3 Meteorological (Precipitation Intensity-Duration, I-D) landslide threshold of Cervinara (**a**) and of Giampilieri (**b**). In the 1000 years long synthetic data set, the red dots represent rainfall events followed by the triggering of a landslide; the blue points are rainfall events after which no landslide was recorded; the power-law red lines, obtained by maximising the true skill statistic (T), so to get the optimal trade-off between missed and false alarms, represent the thresholds separating the two classes of events

Table 5 Performance indicators of the meteorological landslide thresholds for the two tested sites. The thresholds have been obtained by maximising the true skill statistic T for 1000 years long synthetic data sets ($T = 1$ indicates perfect predictions)

Indicator	Cervinara	Giampilieri
Optimal true skill statistic, T	0.934	0.720
Total number of landslides, P	42	231
True alarms, P-M	40	198
Missed alarms, M	2	33
False alarms, F	963	3327

reducing the false alarms would be necessary to ensure a reliable LEWS. Note that the value of the exponent of the I-D threshold is -1. This implies that one of the two rainfall characteristics does not add valuable information for the identification of the threshold, which corresponds to a constant triggering rainfall depth $H = I \times D = 73.3$ mm (indeed, this consideration holds also for Cervinara, although in that case the exponent results slightly different from -1). Nevertheless, in the case of Giampilieri, triggering events with $D > 15$–20 h are no longer aligned with such a line. Probably drainage becomes significant already for relatively short events, owing to the low storage capacity of the soil profile (porosity 0.35), making easier to reach wet conditions.

Hydro-meteorological threshold

To test whether antecedent soil moisture information improves the performance of the thresholds, the best hydro-meteorological thresholds have been identified as power-law equations in the plane (θ, H), by maximizing T. As in real applications, the temporal resolution of moisture measurements is limited and there may be uncertainty in the timing of the landslides, both the near-surface soil moisture (θ_{NS}) and the root-zone soil moisture (θ_{RZ}) have been tested, not only at the onset of the rainfall event but also going backwards, in steps of 24 h, up to 120 h before the beginning of the rainfall.

For Cervinara, the thresholds defined in the (θ_{NS}, H) and (θ_{RZ}, H) planes provide a slight improvement, especially in terms of reducing false alarms (Fig. 4 and Table 6), compared with the ones obtained in the I-D plane (Fig. 3, Table 5). This is especially true if θ_{RZ} is used as a measurement of antecedent soil moisture conditions, as false alarms would be launched once every few years, while nearly all the landslides would be correctly predicted. For Giampilieri, the improved performance of the hydro-meteorological threshold is more evident than for Cervinara. Note that in both cases, soil moisture, either near-surface or root-zone, is representative of conditions predisposing the slope to failure even if it refers to few days before the potentially triggering rainfall events. This is a very important feature, considering the coarseness of the temporal resolution of soil moisture measurements, both for field and remote sensing techniques (e.g. SMOS and SMAP satellites acquire images once every 1 to 3 days). For Cervinara, where the number of landslides is less than 1/1000 of the total observed rainfall events, the threshold corresponding to the maximum T may result too conservative. Indeed, for near-surface soil moisture, the most reliable threshold is identified when antecedent moisture conditions are measured 24 h before rainfall events, minimizing both M and F. Differently, a time lag of

Table 6 Performance indices and values of A and B coefficients of the landslide power-law thresholds. The thresholds have been obtained by maximising the true skill statistic T for 1000 years long synthetic data sets ($T = 1$ indicates perfect predictions). M is the number of missed alarms; F the number of false alarms

Threshold	Time lag [h]	Cervinara					Giampilieri				
		Best T	M	F	A	B	Best T	M	F	A	B
I-D	-	0.934	2	963	175.6	− 1.08	0.720	33	3327	73.31	− 1.00
θ_{NS} - H	0	0.941	2	623	28.11	− 1.71	0.770	14	4116	0.02	− 4.71
	24	0.947	2	301	24.66	− 2.01	0.837	11	2808	0.02	− 4.56
	48	0.946	2	332	26.32	− 1.96	0.857	10	2431	0.06	− 3.96
	72	0.929	2	1252	15.90	− 1.97	0.838	15	2357	0.05	− 4.00
	96	0.933	2	1044	17.72	− 1.96	0.851	13	2261	0.06	− 3.91
	120	0.935	2	935	15.98	− 2.13	0.844	11	2621	0.04	− 4.05
θ_{RZ} - H	0	0.963	1	684	4.08	− 3.98	0.947	1	1170	0.03	− 4.73
	24	0.974	0	1396	0.57	− 5.46	0.943	1	1274	0.04	− 4.56
	48	0.949	2	186	7.84	− 3.96	0.940	3	1129	0.04	− 4.58
	72	0.944	2	461	5.85	− 3.40	0.936	4	1143	0.03	− 4.70
	96	0.946	2	364	6.35	− 3.40	0.921	7	1186	0.11	− 3.89
	120	0.947	2	302	6.17	− 3.50	0.917	4	1593	0.06	− 4.09

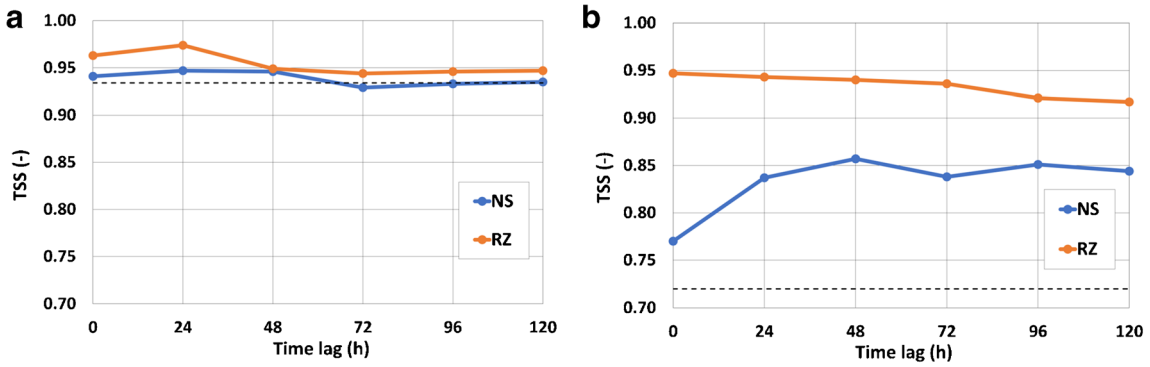

Fig. 4 Optimal T of hydro-meteorological landslide threshold for Cervinara (**a**) and for Giampilieri (**b**). NS indicates near-surface soil moisture (i.e. the upper 5 cm soil layer); RZ indicates root-zone soil moisture (i.e. the upper 1.0 m soil layer); the dashed line indicates the performance of the purely meteorological thresholds. $T = 1$ indicates perfect predictions

48 h seems preferable for root-zone moisture content, as it corresponds to the smallest F with only two missed alarms in 1000 years (Fig. 5 a and b, and Table 6). For Giampilieri, where there is nearly a landslide every 100 rainfall events, the most reliable thresholds are a trade-off between M and F, specifically with θ_{NS} measured 48 h before the rainfall, and θ_{RZ} exactly at the onset of the rainfall events (Fig. 5 c and d, and Table 6). These results clearly indicate that the optimal choice of an empirical thresholds strictly depends on the characteristics of a specific site, namely on the frequency of the feared phenomenon. More rigorously, for practical application in LEWS, the choice should be made quantifying the costs suffered in case of missed activations of the system, as well as the costs related to useless activations.

The slope of the threshold line in the $\log(\theta) - \log(H)$ plane is in all cases very high (i.e. two to five times steeper than the I-D thresholds), indicating that the obtained hydro-meteorological thresholds are very sensitive to both the near-surface and root-zone water content. This shows the information content of antecedent soil moisture for landslide forecasting.

The different behaviour of the two studied sites with respect to slope instability, reflected by the different performances of the obtained thresholds, can be ascribed to differences in both soil hydraulic properties and climate at the two test sites. In Cervinara, owing to the very high storage capacity of the cover and to the precipitations spread throughout the entire year, long-term soil water content fluctuations are relatively limited and typically

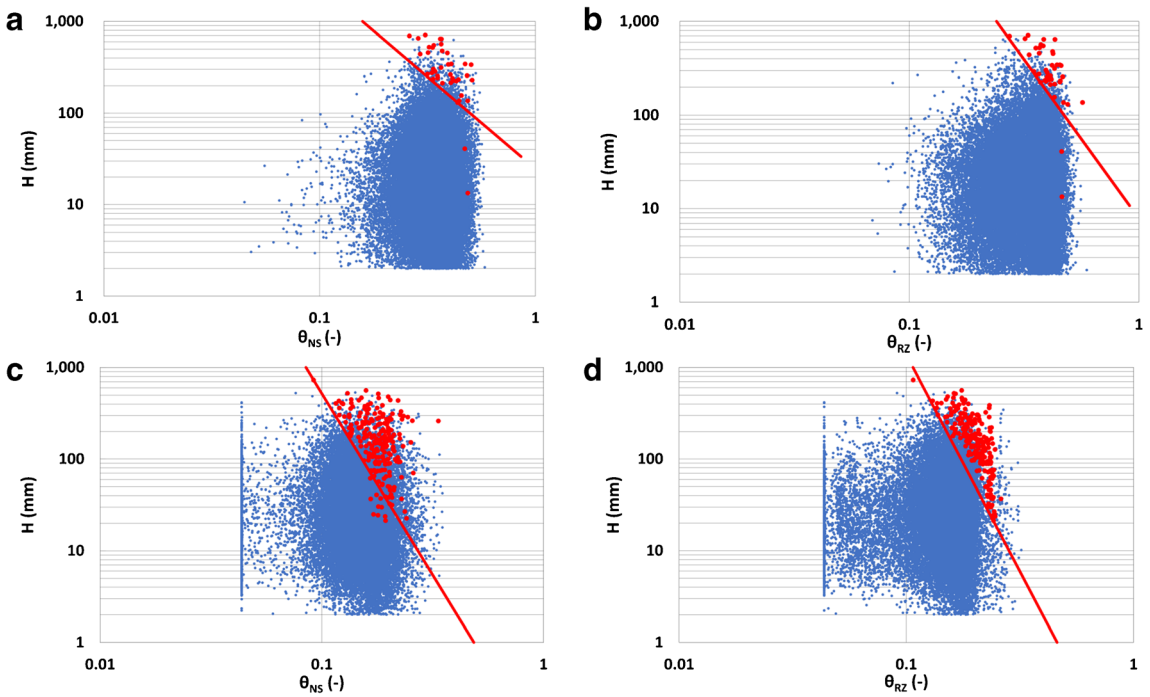

Fig. 5 Optimal hydro-meteorological thresholds for the two tested sites. Data are represented in the (θ, H) plane (θ = soil moisture; H = total event rainfall depth; suffix NS and RZ indicate near surface and root zone soil moisture, respectively). In the 1000 years long synthetic data set, the red dots represent rainfall events followed by the triggering of a landslide; the blue points are rainfall events after which no landslide was recorded; the red power-law lines, obtained by maximising the true skill statistic (T), so to get the optimal trade-off between missed and false alarms, represent the thresholds separating the two classes of events: θ_{NS} with 24 h lead time for Cervinara (**a**); θ_{RZ} with 48 h lead time for Cervinara (**b**); θ_{NS} with 48 h lead time for Giampilieri (**c**); θ_{RZ} at the onset of rainfall for Giampilieri (**d**)

Table 7 Effects of uncertainty in soil moisture measurements on the performance of empirical hydro-meteorological thresholds at the site of Cervinara. The thresholds, identified in the (θ_{NS}, H) plane (θ_{NS} = near surface soil moisture; H = total event rainfall depth), exploit soil water content 24 h before the onset of rainfall events in a 1000 years long synthetic data set. Events followed by the triggering of a landslide have been separated from those after which no landslide was recorded by maximising the true skill statistic (T), so to get the optimal trade-off between missed and false alarms. σ_e is the standard deviation of soil moisture measurement errors; $\overline{\theta}$ the mean water content prior to the onset of rainfall

Error standard deviation, σ_e (m^3 m^{-3})	$\frac{\sigma_e}{\overline{\theta}}$	A	B	T	M	F
0	0	24.7	− 2.01	0.947	2	301
0.01	0.029	23.2	− 1.94	0.944	2	437
0.02	0.059	32.4	− 1.66	0.945	2	383
0.03	0.088	28.4	− 1.66	0.942	2	548
0.04	0.117	29.6	− 1.68	0.944	2	466
0.05	0.147	31.1	− 1.55	0.940	2	633

remain far from soil saturation. In addition, the high hydraulic conductivity makes the infiltration capacity higher than the peak intensity of all rainfall events, preventing overland runoff. Consequently, the attainment of landslide triggering conditions is rare and mostly depends on the total precipitation depth, H, of the triggering event. In Giampilieri, the higher variability of climate forcing, together with the much smaller storage capacity of the cover, enhances the fluctuations of soil water content, favouring the build-up of pore water pressure in response to rainfall events. Furthermore, the smaller hydraulic conductivity, while making the activation of overland runoff more frequent, delays the establishment of leakage through the soil-bedrock interface. Hence, the attainment of landslide triggering conditions depends both on H and on the predisposing soil moisture conditions.

Effects of uncertainty in soil moisture information

All the presented results refer to the "ideal" case in which real values of rainfall, soil moisture, and pore pressure are available, and they all belong exactly to the point of the slope where the landslide prediction should be carried out. In real applications, instead, one should deal with uncertainty in the data, originating from errors in the estimates provided by the available measurement devices, and with variability owing to their spatial and temporal coarse resolution, which in most cases obliges to make use of data collected at some distance (in space and time) from the location and the time at which the prediction is needed. The issue of spatial variability is particularly sensitive for uppermost soil moisture, as it is affected by local factors such as vegetation, soil texture, and drainage conditions.

How uncertainty and variability in rainfall data and landslide inventories may affect *I-D* thresholds has been discussed extensively (e.g. (Berti et al. 2012; Nikolopoulos et al. 2014; Peres et al. 2018; Marra 2019)). Hence, the discussion will be limited here to the effects of the uncertainty of soil moisture information.

All the indirect measurement techniques, either on site or remote, adopted to get estimates of soil water content in the field, rely on a calibration relationship, often non-linear, which may enhance the uncertainty of estimated soil moisture (e.g. (Robinson et al. 2003; Mohanty et al. 2017; Capparelli et al. 2018)).

As the proposed hydro-meteorological thresholds are empirical, i.e. they do not make use of any physically based approach for

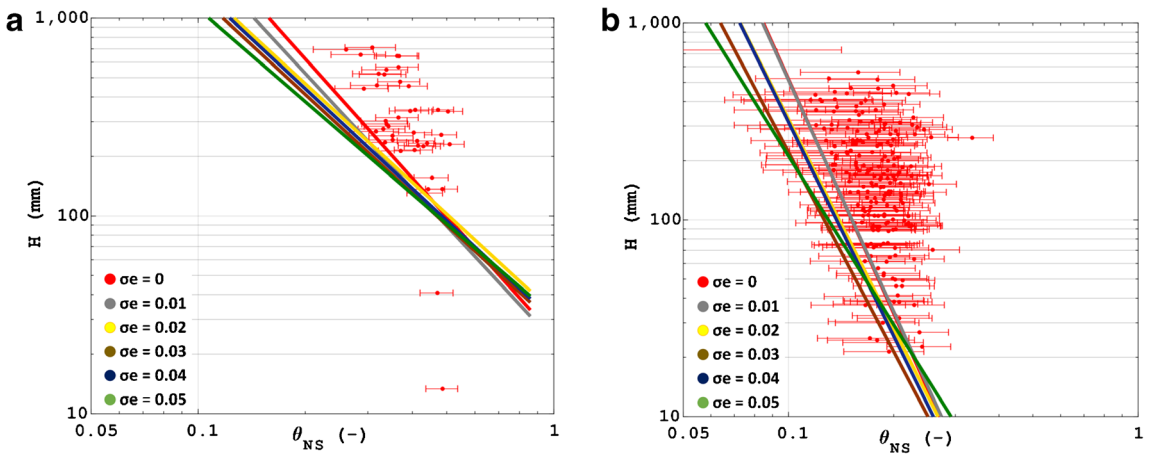

Fig. 6 Effects of uncertainty in soil moisture measurements on optimal hydro-meteorological thresholds for Cervinara (**a**) and Giampilieri (**b**). Data are represented in the (θ_{NS}, H) plane (θ_{NS} = near surface soil moisture; H = total event rainfall depth). In the 1000 years long synthetic data set, the red dots represent rainfall events followed by the triggering of a landslide; the width of the horizontal bars is 0.1, i.e. twice the maximum considered standard deviation of the errors (σ_e = 0.05 m^3 m^{-3}). The power-law lines are obtained by maximising the true skill statistic (T), so to get the optimal trade-off between missed and false alarms for various degrees of uncertainty. They represent the thresholds separating events followed by the triggering of a landslide, from those after which no landslide was recorded

Table 8 Effects of uncertainty in soil moisture measurements on the performance of empirical hydro-meteorological thresholds at the site of Giampilieri. The thresholds, identified in the (θ_{NS}, H) plane (θ_{NS} = near surface soil moisture; H = total event rainfall depth), exploit soil water content 48 h before the onset of rainfall events in a 1000 years long synthetic data set. Events followed by the triggering of a landslide have been separated from those after which no landslide was recorded by maximising the true skill statistic (T), so to get the optimal trade-off between missed and false alarms. σ_e is the standard deviation of soil moisture measurement errors; $\overline{\theta}$ the mean water content prior to the onset of rainfall

Error standard deviation, σ_e (m^3 m^{-3})	$\frac{\sigma_e}{\overline{\theta}}$	A	B	T	M	F
0	0	0.0570	− 3.96	0.857	10	2431
0.01	0.069	0.0632	− 3.91	0.848	12	2435
0.02	0.138	0.0946	− 3.54	0.780	17	3558
0.03	0.207	0.0764	− 3.61	0.754	17	4181
0.04	0.277	0.0940	− 3.37	0.704	16	5492
0.05	0.346	0.299	− 2.85	0.687	28	4654

which the degree of saturation is required, the soil moisture data should be able merely to distinguish wetter from dryer antecedent soil conditions. In this respect, systematic errors or bias in the estimates of soil moisture is not much worrisome, while random errors, if large, may completely change the picture.

So, the robustness of the proposed hydro-meteorological approach to the definition of empirical thresholds for landslide predictions has been tested by assuming that the real values of soil moisture were affected by a Normal-distributed random error with zero mean, the entity of which was characterised by its standard deviation, σ_e. The soil moisture data, provided by the infiltration model (i.e. the "true" soil moisture values), have been perturbed by adding to them random errors, and the hydro-meteorological thresholds for landslide prediction have been identified, on the so obtained "non-ideal" data set, by maximization of T.

The described procedure has been applied to the two examined sites, in both cases with reference to the hydro-meteorological threshold which, making use of near-surface soil moisture, provided the optimal T with the "true" soil moisture data. Specifically, for the case of Cervinara, θ_{NS} acquired 24 h prior the beginning of rainfall events is used (T = 0.947 with "true" data), for Giampilieri, the hydro-meteorological threshold with θ_{NS} acquired 48 h before the beginning of the rainfall events (T = 0.857). Various scenarios have been tested, by considering σ_e varying from 0.01 to 0.05 m^3 m^{-3}. The lower limit can be interpreted as representative of errors of on-site TDR measurements for which a soil-specific calibration relationship has been experimentally determined (Robinson et al. 2003). The upper is the reported uncertainty of the currently available soil moisture retrievals from satellite radar measurements (Chan et al. 2016).

In Cervinara (Fig. 6a), given the high storage capacity of the soil (porosity 0.75), it looks clear that the additional spreading of soil water content data, caused by the introduced random errors, only slightly affects the performance of the threshold, even in the worst analysed scenario, slightly increasing only the number of false alarms. The effect of water content spreading, however, is clearly visible on the inclination of the threshold curves in the log-log plane. In fact, the larger are the errors, the less pronounced is the dependence of the limit rainfall depth H on the initial soil moisture, indicating that the information provided by the initial conditions becomes progressively less significant. Similar effects, but quantitatively larger, are obtained also for Giampilieri (Fig. 6b), likely owing to the smaller storage capacity of the soil (porosity 0.35), which makes larger the impact of moisture measurement errors, leading to a possible increase of false alarms.

Thus, to better quantify the different impacts of soil moisture measurement errors on the two sites, the standard deviation of the errors can be divided by the mean of the water content values preceding all the rainfall events at each site, $\overline{\theta}$.

In Cervinara (Table 7), even in the worst analysed scenario, σ_e does not exceed 15% of the mean pre-event soil water content.

In Giampilieri (Table 8), instead, the errors are relatively larger, with σ_e reaching almost 35% of $\overline{\theta}$, and this affects both the number of false alarms and missed alarms. However, even in the worst scenario, about 88% of the landslides are correctly predicted.

Conclusions

Our study shows the advancements in landslide forecasting that can be achieved by including near surface and root-zone soil moisture, compared with the traditional, and widely used, meteorological thresholds usually in the form of precipitation intensity-duration power-law relationships. The results show that the improvements depend on climate, soil, and geomorphologic features of the area of interest. Specifically, in the case of soils with high water storage and infiltration capacity, the use of soil moisture information can significantly reduce the number of false alarms. This improvement is robust with respect to uncertainty in soil moisture data, such as those coming from remote sensing soil moisture products. In the case of soils with lower storage capacity and hydraulic conductivity, the improvement is even stronger, as both false alarms and missed alarms are reduced, though less robust with respect to uncertainty in soil moisture data. Our analysis also shows that the use of root-zone soil moisture enhances the capability of forecasting shallow landslides more than using near surface soil moisture information only. Good predictive performances are obtained with soil moisture measured 1 to 4 days prior to the onset of a triggering rainfall event, which links with the current remote sensing temporal resolution. This confirms that antecedent soil moisture is an important causal, and dynamic, predisposing factor for landslide initiation, and therefore a key variable to include in shallow landslide forecasting. Our contribution may stimulate a wider use of remotely sensed soil moisture products in landslide forecasting, as their current quality can make landslide early warning

systems more robust, especially for soil covers characterised by small storage capacity. Importantly, we hope our results are a stimulus to continue improving the quality and reliability of remotely sensed near-surface soil moisture measurements as well as root-zone soil moisture estimates, as they could play an important role in regional landslide hazard management.

Acknowledgements

The authors acknowledge the Civil Protection Agency of Campania and Servizio Informativo Agreometeorologico Siciliano (SIAS) for providing rainfall data. The research is part of the Ph.D. project "Modelling hydrological processes affecting rainfall-induced landslides for the development of early warning systems" within the Doctoral Course "A.D.I." of Università degli Studi della Campania "L. Vanvitelli". Most of the work was developed during Marino's 6-month stay as a visiting researcher at the Section Water Resources of Delft University of Technology. The research has been also funded by Università degli Studi della Campania 'L. Vanvitelli' through the programme "VALERE: VAnviteLli pEr la RicErca".

Author contributions

Marino: bibliographic research, numerical experiments, writing (original draft)

Peres: rainfall generation, writing (original draft and review)

Cancelliere: rainfall generation, writing (review)

Greco: analysis of uncertainty, methodology, supervision, writing (original draft and review)

Bogaard: methodology, supervision, writing (original draft and review)

Compliance with ethical standards

Competing interests The authors declare that they have no competing interests.

References

Allocca V, Manna F, De Vita P (2014) Estimating annual groundwater recharge coefficient for karst aquifers of the southern Apennines (Italy). Hydrol Earth Syst Sci 18:803–817. https://doi.org/10.5194/hess-18-803-2014

Al-Yaari A, Wigneron J-P, Ducharne A et al (2014) Global-scale comparison of passive (SMOS) and active (ASCAT) satellite based microwave soil moisture retrievals with soil moisture simulations (MERRA-Land). Remote Sens Environ 152:614–626. https://doi.org/10.1016/j.rse.2014.07.013

Ardizzone F, Basile G, Cardinali M et al (2012) Landslide inventory map for the Briga and the Giampilieri catchments, NE Sicily, Italy. J Maps. https://doi.org/10.1080/17445647.2012.694271

Berti M, Martina MLV, Franceschini S et al (2012) Probabilistic rainfall thresholds for landslide occurrence using a Bayesian approach. J Geophys Res Earth Surf 117:1–20. https://doi.org/10.1029/2012JF002367

Bishop AW (1959) The principle of effective stress. Tek Ukebl

Bisson M, Pareschi MT, Zanchetta G et al (2007) Volcaniclastic debris-flow occurrences in the Campania region (Southern Italy) and their relation to Holocene - Late Pleistocene pyroclastic fall deposits: implications for large-scale hazard mapping. Bull Volcanol. https://doi.org/10.1007/s00445-007-0127-4

Bogaard TA, Greco R (2016) Landslide hydrology: from hydrology to pore pressure. Wiley Interdiscip Rev Water 3:439–459. https://doi.org/10.1002/wat2.1126

Bogaard T, Greco R (2018) Invited perspectives: hydrological perspectives on precipitation intensity-duration thresholds for landslide initiation: proposing hydro-meteorological thresholds. Nat Hazards Earth Syst Sci 18:31–39. https://doi.org/10.5194/nhess-18-31-2018

Bonardi G, de Capoa P, Di Staso A et al (2002) New constraints to the geodynamic evolution of the southern sector of the Calabria–Peloritani Arc (Italy). Compt Rendus Geosci 334:423–430. https://doi.org/10.1016/S1631-0713(02)01729-7

Breznitz S (1984) Cry wolf: The psychology of false alarms. Lawrence Erlbaum Associates, Hillsdale

Brocca L, Ponziani F, Moramarco T et al (2012) Improving landslide forecasting using ASCAT-derived soil moisture data: a case study of the torgiovannetto landslide in central Italy. Remote Sens. https://doi.org/10.3390/rs4051232

Brocca L, Ciabatta L, Moramarco T, et al (2016) Use of satellite soil moisture products for the operational mitigation of landslides risk in Central Italy. In: Satellite soil moisture retrieval: techniques and applications

Cama M, Lombardo L, Conoscenti C et al (2015) Predicting storm-triggered debris flow events: application to the 2009 Ionian Peloritan disaster (Sicily, Italy). Nat Hazards Earth Syst Sci. https://doi.org/10.5194/nhess-15-1785-2015

Capparelli G, Spolverino G, Greco R (2018) Experimental determination of TDR calibration relationship for pyroclastic ashes of campania (Italy). Sensors (Switzerland). https://doi.org/10.3390/s18113727

Chan SK, Bindlish R, O'Neill PE et al (2016) Assessment of the SMAP passive soil moisture product. IEEE Trans Geosci Remote Sens 54:4994–5007. https://doi.org/10.1109/TGRS.2016.2561938

Ciabatta L, Camici S, Brocca L et al (2016) Assessing the impact of climate-change scenarios on landslide occurrence in Umbria Region, Italy. J Hydrol. https://doi.org/10.1016/j.jhydrol.2016.02.007

Comegna L, Damiano E, Greco R et al (2016) Field hydrological monitoring of a sloping shallow pyroclastic deposit. Can Geotech J 53:1125–1137. https://doi.org/10.1139/cgj-2015-0344

Cowpertwait PSP, O'Connell PE, Metcalfe AV, Mawdsley JA (1996) Stochastic point process modelling of rainfall. I Single-site fitting and validation. J Hydrol. https://doi.org/10.1016/S0022-1694(96)80004-7

Crozier MJ (1999) Prediction of rainfall-triggered landslides: a test of the Antecedent Water Status Model. Earth Surf Process Landf 24:825–833. https://doi.org/10.1002/(SICI)1096-9837(199908)24:9<825::AID-ESP14>3.0.CO;2-M

Damiano E, Olivares L (2010) The role of infiltration processes in steep slope stability of pyroclastic granular soils: laboratory and numerical investigation. Nat Hazards 52:329–350. https://doi.org/10.1007/s11069-009-9374-3

Damiano E, Olivares L, Picarelli L (2012) Steep-slope monitoring in unsaturated pyroclastic soils. Eng Geol 137–138:1–12. https://doi.org/10.1016/j.enggeo.2012.03.002

Das NN, Entekhabi D, Dunbar RS et al (2016) Uncertainty estimates in the SMAP combined active-passive downscaled brightness temperature. IEEE Trans Geosci Remote Sens. https://doi.org/10.1109/TGRS.2015.2450694

De Guidi G, Scudero S (2013) Landslide susceptibility assessment in the Peloritani Mts. (Sicily, Italy) and clues for tectonic control of relief processes. Nat Hazards Earth Syst Sci. https://doi.org/10.5194/nhess-13-949-2013

De Jeu RAM, Holmes TRH, Parinussa RM, Owe M (2014) A spatially coherent global soil moisture product with improved temporal resolution. J Hydrol. https://doi.org/10.1016/j.jhydrol.2014.02.015

De Lannoy GJM, Reichle RH (2016) Global assimilation of multiangle and multipolarization SMOS brightness temperature observations into the GEOS-5 catchment land surface model for soil moisture estimation. J Hydrometeorol 17:669–691. https://doi.org/10.1175/JHM-D-15-0037.1

Dumedah G, Walker PJ, Merlin O (2015) Root-zone soil moisture estimation from assimilation of downscaled Soil Moisture and Ocean Salinity data. Adv Water Resour 84:14–22. https://doi.org/10.1016/j.advwatres.2015.07.021

Enrekhabi D, Yueh Si, O'Neil PE et al (2014) SMAP handbook soil moisture active passive mapping soil moisture and freeze/thaw from space

Entekhabi D, Njoku EG, O'Neill PE et al (2010) The soil moisture active passive (SMAP) mission. Proc IEEE 98:704–716. https://doi.org/10.1109/JPROC.2010.2043918

Feddes RA, Kowalik P, Kolinska-Malinka K, Zaradny H (1976) Simulation of field water uptake by plants using a soil water dependent root extraction function. J Hydrol 31:13–26. https://doi.org/10.1016/0022-1694(76)90017-2

Fiorillo F, Guadagno F, Aquino S, De Blasio A (2001) The December 1999 Cervinara landslides: further debris flows in the pyroclastic deposits of Campania (southern Italy). Bull Eng Geol Environ 60:171–184. https://doi.org/10.1007/s100640000093

Ford TW, Quiring SM (2019) Comparison of contemporary in situ, model, and satellite remote sensing soil moisture with a focus on drought monitoring. Water Resour Res. https://doi.org/10.1029/2018WR024039

Ford TW, Harris E, Quiring SM (2014) Estimating root zone soil moisture using near-surface observations from SMOS. Hydrol Earth Syst Sci. https://doi.org/10.5194/hess-18-139-2014

Godt JW, Baum RL, Chleborad AF (2006) Rainfall characteristics for shallow landsliding in Seattle, Washington, USA. Earth Surf Process Landf 31:97–110. https://doi.org/10.1002/esp.1237
Greco R, Gargano R (2015) A novel equation for determining the suction stress of unsaturated soils from the water retention curve based on wetted surface area in pores. Water Resour Res 51:6143–6155. https://doi.org/10.1002/2014WR016541
Greco R, Guida A, Damiano E, Olivares L (2010) Soil water content and suction monitoring in model slopes for shallow flowslides early warning applications. Phys Chem Earth. https://doi.org/10.1016/j.pce.2009.12.003
Greco R, Comegna L, Damiano E et al (2013) Hydrological modelling of a slope covered with shallow pyroclastic deposits from field monitoring data. Hydrol Earth Syst Sci 17:4001–4013. https://doi.org/10.5194/hess-17-4001-2013
Greco R, Marino P, Santonastaso GF, Damiano E (2018) Interaction between perched epikarst aquifer and unsaturated soil cover in the initiation of shallow landslides in pyroclastic soils. Water 10:948. https://doi.org/10.3390/w10070948
Guzzetti F, Peruccacci S, Rossi M, Stark CP (2008) The rainfall intensity–duration control of shallow landslides and debris flows: an update. Landslides 5:3–17. https://doi.org/10.1007/s10346-007-0112-1
Kawanishi T, Sezai T, Ito Y et al (2003) The Advanced Microwave Scanning Radiometer for the Earth observing system (AMSR-E), NASDA's contribution to the EOS for global energy and water cycle studies. IEEE Trans Geosci Remote Sens. https://doi.org/10.1109/TGRS.2002.808331
Kerr YH, Waldteufel P, Richaume P et al (2012) The SMOS soil moisture retrieval algorithm. IEEE Trans Geosci Remote Sens 50:1384–1403. https://doi.org/10.1109/TGRS.2012.2184548
Kirschbaum DB, Adler R, Hong Y, Lerner-Lam A (2009) Evaluation of a preliminary satellite-based landslide hazard algorithm using global landslide inventories. Nat Hazards Earth Syst Sci 9:673–686. https://doi.org/10.5194/nhess-9-673-2009
Kirschbaum DB, Adler R, Hong Y et al (2012) Advances in landslide nowcasting: evaluation of a global and regional modeling approach. Environ Earth Sci 66:1683–1696. https://doi.org/10.1007/s12665-011-0990-3
Kornelsen KC, Coulibaly P (2014) Root-zone soil moisture estimation using data-driven methods. Water Resour Res. https://doi.org/10.1002/2013WR014127
Lazzari M, Piccarreta M, Manfreda S (2018) The role of antecedent soil moisture conditions on rainfall-triggered shallow landslides. Nat Hazards Earth Syst Sci Discuss:1–11. https://doi.org/10.5194/nhess-2018-371
Li F, Crow WT, Kustas WP (2010) Towards the estimation root-zone soil moisture via the simultaneous assimilation of thermal and microwave soil moisture retrievals. Adv Water Resour. https://doi.org/10.1016/j.advwatres.2009.11.007
Li Y, Grimaldi S, Walker JP, Pauwels VRN (2016) Application of remote sensing data to constrain operational rainfall-driven flood forecasting: a review. Remote Sens
Lu N, Godt JW, Wu DT (2010) A closed-form equation for effective stress in unsaturated soil. Water Resour Res. https://doi.org/10.1029/2009wr008646
Lv S, Zeng Y, Wen J et al (2018) Estimation of penetration depth from soil effective temperature in microwave radiometry. Remote Sens 10:519. https://doi.org/10.3390/rs10040519
Manfreda S, Brocca L, Moramarco T et al (2014) A physically based approach for the estimation of root-zone soil moisture from surface measurements. Hydrol Earth Syst Sci. https://doi.org/10.5194/hess-18-1199-2014
Marra F (2019) Rainfall thresholds for landslide occurrence: systematic underestimation using coarse temporal resolution data. Nat Hazards 95:883–890. https://doi.org/10.1007/s11069-018-3508-4
Martens B, Miralles DG, Lievens H et al (2017) GLEAM v3: Satellite-based land evaporation and root-zone soil moisture. Geosci Model Dev. https://doi.org/10.5194/gmd-10-1903-2017
Massari C, Brocca L, Barbetta S et al (2014) Using globally available soil moisture indicators for flood modelling in Mediterranean catchments. Hydrol Earth Syst Sci. https://doi.org/10.5194/hess-18-839-2014
Maugeri M, Motta E (2011) Slope failure. In: Geotechnical, geological and earthquake engineering. pp 169–190
Miralles DG, Holmes TRH, De Jeu RAM et al (2011) Global land-surface evaporation estimated from satellite-based observations. Hydrol Earth Syst Sci. https://doi.org/10.5194/hess-15-453-2011
Mirus B, Morphew M, Smith J (2018) Developing hydro-meteorological thresholds for shallow landslide initiation and early warning. Water 10:1274. https://doi.org/10.3390/w10091274
Mohanty BP, Cosh MH, Lakshmi V, Montzka C (2017) Soil moisture remote sensing: state-of-the-science. Vadose Zo J 16. https://doi.org/10.2136/vzj2016.10.0105
Neyman J, Scott EL (1958) Statistical approach to problems of cosmology. J R Stat Soc Ser B. https://doi.org/10.1111/j.2517-6161.1958.tb00272.x
Nikolopoulos EI, Crema S, Marchi L et al (2014) Impact of uncertainty in rainfall estimation on the identification of rainfall thresholds for debris flow occurrence. Geomorphology 221:286–297. https://doi.org/10.1016/J.GEOMORPH.2014.06.015
Ochsner TE, Cosh MH, Cuenca RH et al (2013) State of the art in large-scale soil moisture monitoring. Soil Sci Soc Am J
Papa MN, Trentini G, Carbone A, Gallo A (2011) An integrated approach for debris flow hazard assessment - a case study on the Amalfi coast - Campania, Italy. In: International Conference on Debris-Flow Hazards Mitigation: Mechanics, Prediction, and Assessment, Proceedings
Parinussa RM, Holmes TRH, Wanders N et al (2015) A preliminary study toward consistent soil moisture from AMSR2. J Hydrometeorol. https://doi.org/10.1175/JHM-D-13-0200.1
Peirce CS (1884) The numerical measure of the success of predictions. Science. https://doi.org/10.1126/science.ns-4.93.453-a
Peng J, Niesel J, Loew A et al (2015) Evaluation of satellite and reanalysis soil moisture products over southwest China using ground-based measurements. Remote Sens. https://doi.org/10.3390/rs71115729
Peres DJ (2013) The hydrologic control on shallow landslide triggering: empirical and Monte Carlo physically-based approaches. University of Catania
Peres DJ, Cancelliere A (2014) Derivation and evaluation of landslide-triggering thresholds by a Monte Carlo approach. Hydrol Earth Syst Sci 18:4913–4931. https://doi.org/10.5194/hess-18-4913-2014
Peres DJ, Cancelliere A (2016) Estimating return period of landslide triggering by Monte Carlo simulation. J Hydrol 541:256–271. https://doi.org/10.1016/j.jhydrol.2016.03.036
Peres DJ, Cancelliere A (2018) Modeling impacts of climate change on return period of landslide triggering. J Hydrol 567:420–434. https://doi.org/10.1016/J.JHYDROL.2018.10.036
Peres DJ, Cancelliere A, Greco R, Bogaard TA (2018) Influence of uncertain identification of triggering rainfall on the assessment of landslide early warning thresholds. Nat Hazards Earth Syst Sci 18:633–646. https://doi.org/10.5194/nhess-18-633-2018
Ponziani F, Pandolfo C, Stelluti M et al (2012) Assessment of rainfall thresholds and soil moisture modeling for operational hydrogeological risk prevention in the Umbria region (central Italy). Landslides 9:229–237. https://doi.org/10.1007/s10346-011-0287-3
Ragab R (1995) Towards a continuous operational system to estimate the root-zone soil moisture from intermittent remotely sensed surface moisture. J Hydrol. https://doi.org/10.1016/0022-1694(95)02749-F
Rao KS, Chandra G, Narasimha Rao PV (1988) Study on penetration depth and its dependence on frequency, soil moisture, texture and temperature in the context of microwave remote sensing. J Indian Soc Remote Sens 16:7–19. https://doi.org/10.1007/BF03014300
Ray RL, Jacobs JM (2007) Relationships among remotely sensed soil moisture, precipitation and landslide events. Nat Hazards 43:211–222. https://doi.org/10.1007/s11069-006-9095-9
Ray RL, Jacobs JM, Cosh MH (2010) Landslide susceptibility mapping using downscaled AMSR-E soil moisture: a case study from Cleveland Corral, California, US. Remote Sens Environ 114:2624–2636. https://doi.org/10.1016/j.rse.2010.05.033
Ray RL, Fares A, He Y, Temimi M (2017) Evaluation and inter-comparison of satellite soil moisture products using in situ observations over Texas, U.S. Water (Switzerland). https://doi.org/10.3390/w9060372
Richards LA (1931) Capillary conduction of liquids through porous mediums. J Appl Phys. https://doi.org/10.1063/1.1745010
Robinson DA, Jones SB, Wraith JM et al (2003) A review of advances in dielectric and electrical conductivity measurement in soils using time domain reflectometry. Vadose Zo J. https://doi.org/10.2113/2.4.444
Rodriguez-Iturbe I, Febres De Power B, Valdes JB (1987) Rectangular pulses point process models for rainfall: analysis of empirical data. J Geophys Res. https://doi.org/10.1029/JD092iD08p09645
Rolandi G, Bellucci F, Heizler MT et al (2003) Tectonic controls on the genesis of ignimbrites from the Campanian Volcanic Zone, southern Italy. Mineral Petrol 79:3–31. https://doi.org/10.1007/s00710-003-0014-4
Sabater JM, Jarlan L, Calvet J-C et al (2007) From near-surface to root-zone soil moisture using different assimilation techniques. J Hydrometeorol. https://doi.org/10.1175/jhm571.1
Schaap MG, Leij FJ, Van Genuchten MT (2001) Rosetta: a computer program for estimating soil hydraulic parameters with hierarchical pedotransfer functions. J Hydrol. https://doi.org/10.1016/S0022-1694(01)00466-8
Schilirò L, Esposito C, Scarascia Mugnozza G (2015) Evaluation of shallow landslide-triggering scenarios through a physically based approach: an example of application in the southern Messina area (northeastern Sicily, Italy). Nat Hazards Earth Syst Sci. https://doi.org/10.5194/nhess-15-2091-2015
Schmugge T (1998) Applications of passive microwave observations of surface soil moisture. J Hydrol 212–213:188–197. https://doi.org/10.1016/S0022-1694(98)00209-1
Schmugge TJ, Jackson TJ, McKim HL (1980) Survey of methods for soil moisture determination. Water Resour Res 16:961–979. https://doi.org/10.1029/WR016i006p00961

Segoni S, Rosi A, Lagomarsino D et al (2018) Brief communication: Using averaged soil moisture estimates to improve the performances of a regional-scale landslide early warning system. Nat Hazards Earth Syst Sci. https://doi.org/10.5194/nhess-18-807-2018

Shravan Kumar Yadav SR, Roy SS (2013) Remote sensing technology and its applications. Int J Adv Res Technol 2:25–30

Shuttleworth WJ (1993) Evaporation. In: Maidment DR (ed) Handbook of hydrology. McGraw-Hill, New York

Šimůnek J, van Genuchten MT, Šejna M (2008) Development and applications of the HYDRUS and STANMOD software packages and related codes. Vadose Zo J 7:587. https://doi.org/10.2136/vzj2007.0077

Stähli M, Sättele M, Huggel C et al (2015) Monitoring and prediction in early warning systems for rapid mass movements. Nat Hazards Earth Syst Sci 15:905–917. https://doi.org/10.5194/nhess-15-905-2015

Stancanelli LM, Peres DJ, Cancelliere A, Foti E (2017) A combined triggering-propagation modeling approach for the assessment of rainfall induced debris flow susceptibility. J Hydrol. https://doi.org/10.1016/j.jhydrol.2017.04.038

Thomas MA, Collins BD, Mirus BB (2019) Assessing the feasibility of satellite-based thresholds for hydrologically driven landsliding. Water Resour Res. https://doi.org/10.1029/2019WR025577

van Genuchten MT (1980) A closed-form equation for predicting the hydraulic conductivity of unsaturated soils1. Soil Sci Soc Am J 44:892. https://doi.org/10.2136/sssaj1980.03615995004400050002x

Vignaroli G, Rossetti F, Theye T, Faccenna C (2008) Styles and regimes of orogenic thickening in the Peloritani Mountains (Sicily, Italy): new constraints on the tectono-metamorphic evolution of the Apennine belt. Geol Mag. https://doi.org/10.1017/S0016756807004293

Wagner W, Lemoine G, Rott H (1999) A method for estimating soil moisture from ERS scatterometer and soil data. Remote Sens Environ. https://doi.org/10.1016/S0034-4257(99)00036-X

Wagner W, Hahn S, Kidd R et al (2013) The ASCAT soil moisture product: a review of its specifications, validation results, and emerging applications. Meteorol. Zeitschrift

Walker JP, Willgoose GR, Kalma JD (2002) Three-dimensional soil moisture profile retrieval by assimilation of near-surface measurements: simplified Kalman filter covariance forecasting and field application. Water Resour Res. https://doi.org/10.1029/2002wr001545

Walker JP, Willgoose GR, Kalma JD (2004) In situ measurement of soil moisture: a comparison of techniques. J Hydrol 293:85–99. https://doi.org/10.1016/j.jhydrol.2004.01.008

Wanders N, Karssenberg D, De Roo A et al (2014) The suitability of remotely sensed soil moisture for improving operational flood forecasting. Hydrol Earth Syst Sci. https://doi.org/10.5194/hess-18-2343-2014

Zhao B, Dai Q, Han D et al (2019) Probabilistic thresholds for landslides warning by integrating soil moisture conditions with rainfall thresholds. J Hydrol. https://doi.org/10.1016/j.jhydrol.2019.04.062

Zhuo L, Dai Q, Han D et al (2019) Evaluation of remotely sensed soil moisture for landslide hazard assessment. IEEE J Sel Top Appl Earth Obs Remote Sens. https://doi.org/10.1109/JSTARS.2018.2883361

P. Marino (✉) · **R. Greco**
Dipartimento di ingegneria,
Università degli Studi della Campania "Luigi Vanvitelli",
via Roma 9, 81031, Aversa, CE, Italy
Email: pasquale.marino1@unicampania.it

R. Greco
e-mail: roberto.greco@unicampania.it

D. J. Peres · **A. Cancelliere**
Department of Civil Engineering and Architecture,
University of Catania,
95123, Catania, Italy

D. J. Peres
e-mail: djperes@dica.unict.it

A. Cancelliere
e-mail: antonino.cancelliere@unict.it

T. A. Bogaard
Section Water Resources, Department of Water Management, Faculty of Civil Engineering and Geosciences,
Delft University of Technology,
PO Box 50482600 GA, Delft, The Netherlands
e-mail: T.A.Bogaard@tudelft.nl